Journal of Materials Chemistry A

COMMUNICATION

View Article Online
View Journal | View Issue

Cite this: J. Mater. Chem. A, 2016, 4, 10135

Received 14th May 2016
Accepted 6th June 2016

DOI: 10.1039/c6ta04030f

www.rsc.org/MaterialsA

Efficient polymer solar cells based on a copolymer of *meta*-alkoxy-phenyl-substituted benzodithiophene and thieno[3,4-*b*]thiophene†

Wanbin Li,[a] Bing Guo,[a] Chunmei Chang,[a] Xia Guo,*[a] Maojie Zhang*[a] and Yongfang Li*[ab]

A new conjugated copolymer, **PBTF-OP**, based on *meta*-alkoxy-phenyl-substituted benzodithiophene (BDT-*m*-OP) and 2-ethylhexyl-3-fluorothieno[3,4-*b*]thiophene-2-carboxylate (TT) was designed and synthesized for application as the donor material in polymer solar cells (PSCs). **PBTF-OP** possesses a similar molecular structure to the well-known polymer **PTB7-Th** but different conjugated side chains on the BDT unit: *meta*-alkoxy-phenyl side chains for **PBTF-OP** and alkylthienyl side chains for **PTB7-Th**. Compared with **PTB7-Th**, **PBTF-OP** exhibits absorption with some blue shifts, while it possesses a deeper HOMO energy level of −5.45 eV and a slightly enhanced hole mobility of 1.25×10^{-3} cm^2 (V^{-1} s^{-1}) *versus* a HOMO energy level of −5.30 eV and a hole mobility of 1.11×10^{-3} cm^2 (V^{-1} s^{-1}) for **PTB7-Th**. The PSCs based on **PBTF-OP**:$PC_{71}BM$ showed a higher power conversion efficiency (PCE) of 9.0% with a higher V_{oc} of 0.86 V in comparison with a PCE of 8.3% and a V_{oc} of 0.78 V for **PTB7-Th**. The results indicate that side chain engineering of BDT-based copolymers is an effective way to improve photovoltaic performance of polymer donors.

Introduction

Bulk heterojunction (BHJ) polymer solar cells (PSCs) have attracted great attention for applications in renewable energy due to their advantages of low cost, easy fabrication, light weight and capability to be fabricated into large area flexible devices.[1–5] The photoactive blend layer of the PSCs, which is sandwiched between an anode and a cathode, is composed of a conjugated polymer as the donor and a fullerene derivative as the acceptor.[6,7] As is well known, the power conversion efficiency (PCE) of PSCs is determined by three key factors: open-circuit voltage (V_{oc}), short-circuit current density (J_{sc}) and fill factor (FF).[8–10] These parameters are closely related to the optical and electrical properties of the polymer donors and the blend morphology of the active layer in the PSCs. Consequently, a promising polymer donor material should possess broad and strong absorption in order to obtain high J_{sc}, high hole mobility to achieve high FF, and a suitable molecular energy level matching that of the fullerene derivative acceptor to achieve high V_{oc}.[11] In addition, it is also essential for the polymer donor materials to feasibly form the optimal nano-scaled morphology in the blend film with the acceptor.[12,13] Hence, main chain engineering (such as donor–acceptor (D–A) copolymerization) and side chain engineering (such as the conjugated side chain and electron withdrawing side chain) have been performed to tune the absorption, electronic energy levels and charge carrier mobility of the conjugated polymers. Recently, great progress has been achieved with a PCE over 10% for the PSCs based on narrow bandgap polymers as donors.[14–19]

Among various polymer donor materials, two-dimension (2D)-conjugated polymers based on benzodithiophene (BDT) with conjugated side chains exhibit superior photovoltaic performance due to their extended conjugation and enhanced intermolecular π–π interactions, which result in broader absorption and higher hole mobility.[20–26] In addition, the molecular energy levels of the polymers can be effectively modulated by choosing suitable conjugated side chains.[26] It is well known that the V_{oc} of the PSCs is proportional to the energy gap between the highest occupied molecular orbital (HOMO) level of the polymer donor and the lowest unoccupied molecular orbital (LUMO) level of the acceptor.[27–29] The modification of conjugated side chains of the 2D-conjugated polymers has been confirmed to be an effective way to improve the V_{oc} and hence the PCE of the PSCs based on the 2D BDT-based polymers. For example, in our previous work,[30] two polymers **PBT-OP** and **PBT-T** were designed and synthesized, based on BDT with *meta*-alkoxy-phenyl side groups (BDT-*m*-OP) or alkylthienyl side groups (**BDT-T**), respectively. It can be found that the variation of side chains has a significant impact on the polymer's HOMO levels. From **PBT-T** to **PBT-OP**, the HOMO energy level

[a]Laboratory of Advanced Optoelectronic Materials, College of Chemistry, Chemical Engineering and Materials Science, Soochow University, Suzhou 215123, China. E-mail: mjzhang@suda.edu.cn; guoxia@suda.edu.cn

[b]Beijing National Laboratory for Molecular Sciences, CAS Key Laboratory of Organic Solids, Institute of Chemistry, Chinese Academy of Sciences, Beijing 100190, China. E-mail: liyf@iccas.ac.cn

† Electronic supplementary information (ESI) available. See DOI: 10.1039/c6ta04030f

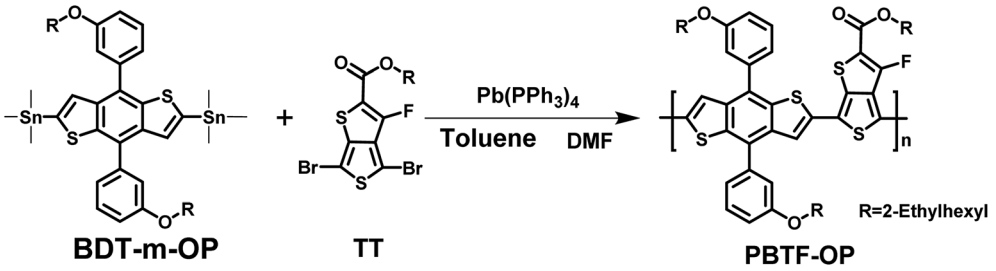

Scheme 1 Synthetic route and molecular structure of PBTF-OP.

decreased by 0.25 eV, the V_{oc} of PSCs increased from 0.60 V to 0.78 V, and the final PCE of the PSCs based on **PBT-OP** increased by ~36% compared with that of the devices based on **PBT-T**. Therefore, BDT with *meta*-alkoxy-phenyl side groups is an effective building block for promising donor materials with high V_{oc}.

In this work, we synthesized a new copolymer **PBTF-OP** (as shown in Scheme 1), based on the *meta*-alkoxy-phenyl-substituted BDT (BDT-*m*-OP) and 2-ethylhexyl-3-fluorothieno [3,4-*b*]thiophene-2-carboxylate (TT) units. The optical, electrochemical and photovoltaic properties of the polymer were systematically investigated. Compared with the analogue polymer **PTB7-Th** based on **BDT-T**, **PBTF-OP** exhibits an absorption spectrum with some blue shift, while it possesses a deeper HOMO energy level of −5.45 eV and a slightly enhanced hole mobility of 1.25×10^{-3} cm^2 (V^{-1} s^{-1}) *versus* a HOMO of −5.30 eV and a hole mobility of 1.11×10^{-3} cm^2 (V^{-1} s^{-1}) for **PTB7-Th**. The PSCs based on **PBTF-OP**:$PC_{71}BM$ showed a higher PCE of 9.0% with a higher V_{oc} of 0.86 V in comparison with a PCE of 8.3% and V_{oc} of 0.78 V for **PTB7-Th**, which indicates that **PBTF-OP** will be a promising polymer donor material for PSCs.

Results and discussion

The synthetic route of **PBTF-OP** is shown in Scheme 1. The monomer BDT-*m*-OP was synthesized according to a previously reported procedure.[30,31] **PBTF-OP** was synthesized using a Pd-catalyzed Stille-coupling reaction. The polymer exhibits good solubility in chloroform, chlorobenzene, and *o*-dichlorobenzene (*o*-DCB). The number average molecular weight (M_n) and polydispersity index (PDI) of **PBTF-OP** and **PTB7-Th** were measured using gel-permeation chromatography (GPC) with 1,2,4-tricholorobenzene as the solvent and polystyrene as a standard at a high temperature of 160 °C. The thermal stability of the polymer was evaluated by thermogravimetric analysis (TGA) and the TGA plot is shown in Fig. 1. The onset of decomposition temperature (T_d) at 5% weight loss is *ca.* 390 °C, indicating that the thermal stability of the polymer is good enough for application as a photovoltaic material in PSCs.

Fig. 2a shows the absorption spectra of **PBTF-OP** and **PTB7-Th** (for comparison) in thin solid film, and the absorption spectra of their solutions in *o*-dichlorobenzene are shown in Fig. S1 in the ESI.† The detailed data of the optical properties of the two polymers are summarized in Table 1 for a clear comparison. In solution, **PBTF-OP** shows two distinct

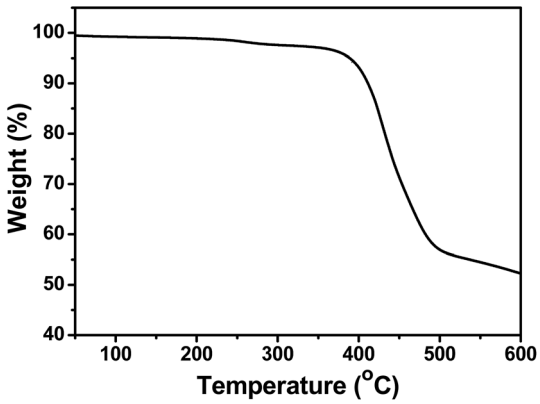

Fig. 1 TGA plot of PBTF-OP with a heating rate of 10 °C min under an inert atmosphere.

absorption bands in a short wavelength range of 300–400 nm and in a long wavelength range of 400–750 nm, which can be ascribed to the π–π* transitions of the backbone and the intramolecular charge-transfer (ICT) of the polymer, respectively. The maximum absorption peak is located at 612 nm and a shoulder peak is at 674 nm. **PBTF-OP** in a solid film exhibits a slightly red-shifted absorption spectrum with a stronger shoulder peak due to the enhanced aggregation of the polymer chains in the solid state in comparison with that in solution. Compared with **PTB7-Th**, the absorption spectrum of **PBTF-OP** exhibits obvious blue-shifts both in solution and in solid film. The absorption peak of **PBTF-OP** film is at 674 nm in comparison with that (702 nm) of **PTB7-Th** film, which can be ascribed to the weaker electron-donating ability of the phenyl side chains in **PBTF-OP** in comparison with the thienyl side chains in **PTB7-Th**.[32] The absorption edge (λ_{edge}) of **PBTF-OP** films is at 766 nm which corresponds to an optical energy bandgap (E_g^{opt}) of 1.62 eV according to $E_g^{opt} = 1240/\lambda_{edge}$. In comparison, λ_{edge} of **PTB7-Th** films is at 790 nm corresponding to an E_g^{opt} of 1.57 eV.

Electrochemical cyclic voltammetry (CV) was performed to measure the electronic energy levels of the two polymers. As shown in Fig. 2b, the onset oxidation potentials (φ_{ox}) of **PTB7-Th** and **PBTF-OP** are 0.60 V and 0.74 V *vs.* Ag/Ag$^+$, while their onset reduction potential (φ_{red}) is −1.38 V and −1.37 V *vs.* Ag/Ag$^+$, respectively. According to the equations,[33,34] HOMO $= -e(\varphi_{ox} + 4.71)$ (eV) and LUMO $= -e(\varphi_{red} + 4.71)$ (eV), the HOMO/LUMO energy levels were calculated from the onset oxidation/reduction potentials. The LUMO levels of **PTB7-Th** and **PBTF-OP** are

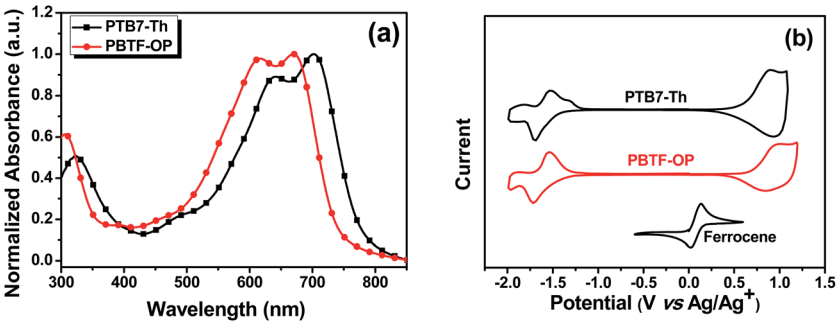

Fig. 2 (a) UV-vis absorption spectra of PBTF-OP and PTB7-Th films; (b) cyclic voltammograms of the polymer films on a platinum electrode measured in 0.1 mol L^{-1} Bu_4NPF_6 acetonitrile solution at a scan rate of 50 mV s^{-1}.

Table 1 Optical properties and electronic energy levels of PBTF-OP film in comparison with those of PTB7-Th film

Polymer	λ_{max} (film) (nm)	λ_{onset} (film) (nm)	E_g^{opt} (eV)	HOMO[a] (eV)	LUMO[a] (eV)	LUMO[b] (eV)	HOMO[b] (eV)
PBTF-OP	612/674	766	1.62	−5.45	−3.34	−2.06	−5.12
PTB7-Th	638/702	790	1.57	−5.30	−3.33	−2.07	−5.07

[a] Calculated from the cyclic voltammograms. [b] Obtained by DFT theoretical calculations.

−3.33 eV and −3.34 eV and their HOMO levels are −5.30 eV and −5.45 eV, respectively. Compared with **PTB7-Th**, the HOMO energy level of **PBTF-OP** is down-shifted by 0.15 eV, which is beneficial for higher V_{oc} of the PSCs with the polymer as the donor, since the V_{oc} of PSCs is proportional to the difference of the LUMO level of the electron acceptor and the HOMO level of the electron donor.

Furthermore, theoretical calculation by density functional theory (DFT) was carried out to evaluate the influence of conjugated side chains on the electronic properties and energy levels of the two polymers. To simplify the calculation, we replaced the long side chains by methyl groups. The calculated frontier molecular orbitals are shown in Fig. S2 in the ESI† and the corresponding HOMO and LUMO levels are also listed in Table 1. The HOMO surfaces of the polymers are delocalized along the whole π-conjugated backbones, while their LUMO surfaces mainly localized on TT acceptor units and partially delocalized on the BDT donor segment. The variation trend of energy levels is consistent with the results from the CV measurements.

X-ray diffraction (XRD) measurements were performed to study the crystallinity of the polymers. Fig. 3 shows the XRD patterns of **PBTF-OP** and **PTB7-Th** films cast from *o*-DCB. The film of **PBTF-OP** showed pronounced (100, 200) diffraction peaks at $2\theta = 5.4°$ and 10.6°, respectively, arising from the alkyl chain packing with the *d*-spacing of ~16.4 Å. In contrast, the film of **PTB7-Th** exhibited weak diffraction peaks located at similar positions as those of **PBTF-OP**. Furthermore, both polymers exhibited strong diffraction peaks at $2\theta = 22.6°$, corresponding to the (010) π–π stacking with the *d*-spacing of 3.9 Å. These results indicate that alkoxyphenyl-conjugated side chains instead of alkylthienyl-conjugated side chains in **PBTF-OP** were beneficial for the ordered molecular packing.

Hole mobilities of **PBTF-OP** along with **PTB7-Th** for comparison were also measured by the space-charge limited current (SCLC) method with a device structure of ITO/PEDOT:PSS/polymer/Au, and the corresponding plots are shown in Fig. S3 in the ESI.† The hole mobility of **PBTF-OP** is 1.25×10^{-3} cm^2 V^{-1} s^{-1} which is slightly higher than that of **PTB7-Th** (1.11×10^{-3} cm^2 V^{-1} s^{-1}).

PSCs with the device structure of ITO/PEDOT:PSS/polymer:$PC_{71}BM$/Ca/Al were fabricated and characterized to investigate the photovoltaic performance of the polymer. First, the D/A (**PBTF-OP**:$PC_{71}BM$) weight ratios in the blend active layer of the devices were optimized. The current density–voltage (*J*–*V*) curves of the devices under AM 1.5 G illumination (100 mW cm^{-2}) and the external quantum efficiency (EQE) spectra of the devices with different D/A ratios (1 : 1, 1 : 1.5 and 1 : 2, w/w)

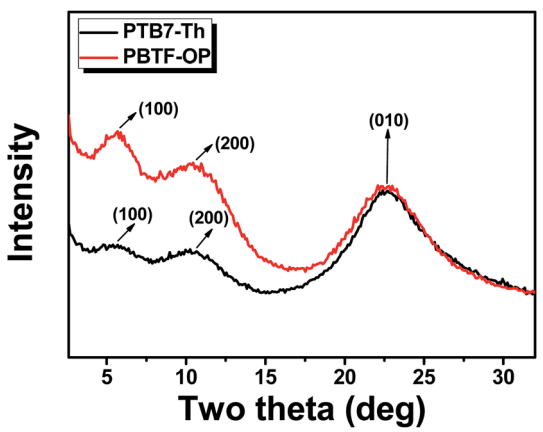

Fig. 3 X-ray diffraction patterns of PBTF-OP and PTB7-Th films cast from *o*-DCB on Si substrates.

are shown in Fig. S4 in the ESI.† We found that the optimal D/A weight ratio is 1 : 1.5.

In order to optimize the morphologies of the blend films and thus to improve their photovoltaic properties, 1,8-diiodooctane (DIO) was used as an additive.[35–37] Fig. 4a and b show the *J*–*V* curves of the PSCs based on polymer : $PC_{71}BM$ (1 : 1.5, w/w) with a different content of DIO as the solvent additive under AM 1.5G illumination (100 mW cm^{-2}) and the external quantum efficiency (EQE) curves of the corresponding devices, respectively. The corresponding photovoltaic parameters of the devices are summarized in Table 2. It can be seen that the devices processed with the DIO additive showed an enhanced J_{sc} and FF and a slightly decreased V_{oc} in comparison with the device without additive processing, which could be ascribed to the variation of surface composition and the bulk morphology of the blend films.[38] When 1.5% DIO additive was used, the devices based on **PBTF-OP**:$PC_{71}BM$ exhibited a maximum PCE of 9.0% with V_{oc} = 0.86 V, J_{sc} = 16.5 mA cm^{-2} and FF = 63.2%. As shown in Fig. 4b, the EQE curves of all the devices cover a broad wavelength range of 300–750 nm. When adding 1.5% DIO as the solvent additive, the EQE of the device enhanced remarkably in the wavelength range from 400 nm to 750 nm. The integral current density values deduced from the EQE curves and the standard solar spectrum (AM 1.5G), as also listed in Table 2, agree well with the J_{sc} values obtained from the *J*–*V* measurement, within 2–3% mismatch. In addition, the PSCs based on **PTB7-Th**:$PC_{71}BM$ were also fabricated under the same conditions, and their photovoltaic performances are also shown in Fig. 4 and listed in Table 2 for comparison. The PSCs based on **PTB7-Th**:$PC_{71}BM$ with the treatment of 1.5% DIO solvent additive showed a PCE of 7.7% with V_{oc} = 0.78 V, J_{sc} = 16.0 mA cm^{-2} and FF = 60.9%. For the optimized device with the treatment of 3% DIO additive, the PCE reached 8.3% with V_{oc} = 0.78 V, J_{sc} = 17.1 mA cm^{-2} and FF = 62.4%, which are similar to the results reported in the literature.[39] Hence, by replacing alkylthienyl groups in **PTB7-Th** with *meta*-alkoxyphenyl groups in **PBTF-OP**, the V_{oc} of the PSCs increased by 0.08 V, while the J_{sc} and FF changed little; the final PCE increased from 8.3% to 9.0%. Considering that the molecular weight of the polymer has a great influence on the device performance, two other batches of **PBTF-OP** and **PTB7-Th** with different molecular weights were synthesized as shown in Fig. S5 and Table S1 in the ESI.† The corresponding PSCs were fabricated according to the above optimized conditions. The *J*–*V* curves and EQE spectra of the devices are shown in Fig. S6 in the ESI.† The photovoltaic parameters of the devices are summarized in Table S1 in the ESI.† It can be seen that all the devices based on **PBTF-OP** exhibited better performance than the PSCs based on **PTB7-Th** with different molecular weights.

For explaining the effect of the DIO additive concentration on the photovoltaic performance of the PSCs, we measured the XRD patterns of the blend films of **PBTF-OP** : $PC_{71}BM$ (1 : 1.5, w/w) with different contents of DIO as the solvent additive, as shown in Fig. S7 in the ESI.† The blend film of **PBTF-OP**:$PC_{71}BM$ with the treatment of 1.5% DIO additive showed the pronounced (100) diffraction peak and (010) diffraction peak of **PBTF-OP** at $2\theta = 4.8°$ and 19.5°, respectively, corresponding to the *d*-spacing of 18.4 Å and 4.5 Å, respectively. In contrast, the blend film of **PTB7-Th**:$PC_{71}BM$ with the treatment of 3% DIO additive exhibited a weaker (100) diffraction peak at $2\theta = 4.3°$ and a (010) diffraction peak at $2\theta = 19.5°$ corresponding to the *d*-spacing of 20.5 Å and 4.5 Å, respectively. The more ordered

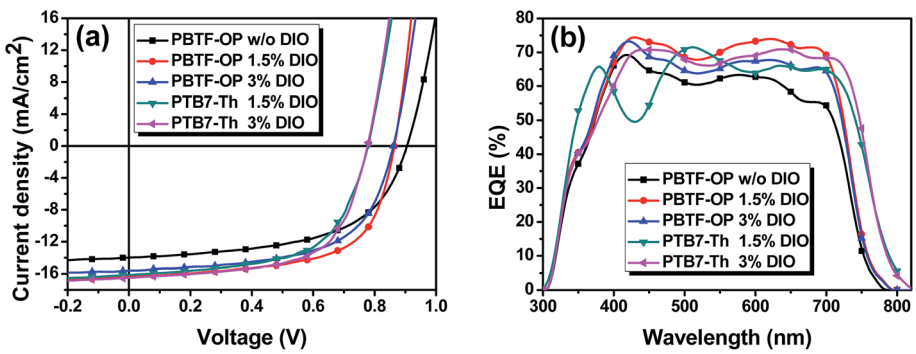

Fig. 4 (a) *J*–*V* curves of the PSCs based on polymer : $PC_{71}BM$ (1 : 1.5, w/w) under AM 1.5G illumination, 100 mW cm^{-2} (b) EQE curves of the corresponding devices.

Table 2 Photovoltaic performances of the PSCs based on polymer : $PC_{71}BM$ (1 : 1.5, w/w) under AM1.5G illumination (100 mW cm^{-2})

Polymers	Conditions	V_{oc} (V)	J_{sc} (mA cm^{-2})	J_{sc}[a] (mA cm^{-2})	FF (%)	PCE_{ave}[b] (%)	PCE_{max} (%)	Thickness (nm)
PBTF-OP	w/o	0.90 (±0.001)	13.9 (±0.2)	13.7	56.7 (±1.0)	7.0 (±0.1)	7.1	95
	1.5% DIO	0.86 (±0.001)	16.4 (±0.2)	16.1	62.2 (±1.0)	8.9 (±0.1)	9.0	105
	3% DIO	0.86 (±0.001)	15.4 (±0.3)	15.1	60.4 (±2.0)	7.9 (±0.1)	8.1	108
PTB7-Th	1.5% DIO	0.78 (±0.001)	16.0 (±0.2)	15.7	60.9 (±2.0)	7.5 (±0.1)	7.7	102
	3% DIO	0.78 (±0.001)	16.9 (±0.3)	16.6	61.4 (±1.0)	8.2 (±0.1)	8.3	105

[a] Values calculated by EQE. [b] The average PCE is obtained from over 20 devices.

molecular packing of **PBTF-OP** in the blend film with the DIO additive treatment is beneficial for the better charge transportation and the improved photovoltaic performance.

To investigate the effect of the morphology on the device performance, the surface and bulk morphologies of the blend films were characterized using atomic force microscopy (AFM) and transmission electron microscopy (TEM). According to the AFM images shown in Fig. S8 in the ESI,† the root-mean-square (RMS) roughness is 0.89 nm, 1.48 nm and 1.63 nm for the blend films processed without additive, with 1.5% DIO and with 3% DIO additive, respectively, indicating that the phase separation of the blend was enhanced with the increase of the additive amount. As shown in the TEM images in Fig. 5, the blend films processed with 1.5% DIO as the additive exhibited a clear continuous fibrillar network with the suitable phase separation and domain size, which are beneficial for the exciton separation and charge transportation in the blend film.

In addition, the electron and hole mobilities of the blend films processed without or with 1.5% DIO additive were measured by using the space charge limited current (SCLC) method. As shown in Fig. S9 and Table S2 in the ESI,† the blend film with DIO treatment exhibited higher hole and electron mobilities and more balanced charge transport than the blend film cast from DCB, which is beneficial for the higher J_{sc} and FF. These results are consistent with variation of photovoltaic performance of the corresponding devices.

In conclusion, a new 2D-conjugated copolymer based on BDT-*m*-OP and TT units, **PBTF-OP**, was designed and synthesized for application as donors in PSCs. The absorption spectra, electronic energy levels and photovoltaic properties of the polymer were characterized. Compared with **PTB7-Th**, **PBTF-OP** exhibited a more deeper HOMO level of −5.45 eV and a slightly higher hole mobility, despite the blue-shifted absorption spectra. The optimized PSCs based on **PBTF-OP**:$PC_{71}BM$ showed a PCE of 9.0% *versus* 8.3% of **PTB7-Th** with the same device structure. The results indicate that **PBTF-OP** will be a promising donor material for high performance PSCs.

Experimental section

Chemicals

The chemical raw materials were purchased from Aldrich, TCI Chemical, J&K and Alfa Aesar, respectively, which were of reagent grade and used without further purification. $PC_{71}BM$ was purchased from Solarmer Materials Inc. The monomer (BDT-*m*-OP) was synthesized according to previously reported procedures.[30,31] The monomer (TT) was purchased from Suna Tech Inc.

Synthesis of the polymer PBTF-OP

In a 50 mL round bottom flask, BDT-*m*-OP and TT were dissolved in 10 mL toluene and 2 mL DMF. After being flushed with argon for 20 min, 17 mg of $Pd(PPh_3)_4$ was added into the flask as the catalyst, and then the mixture was flushed with argon for another 30 min. The solution was stirred at 110 °C for 13 hours under an argon atmosphere and the reactant was cooled down to room temperature, and the polymer was precipitated into 100 mL of methanol. The polymer was collected by filtration and subjected to Soxhlet extraction with methanol, hexane, and chloroform in the end. The solution was evaporated under reduced pressure and precipitated into 100 mL of methanol. The polymer was collected by filtration and dried under vacuum. Three batches of polymers with different molecular weights were obtained by tuning the polymerization time. Anal. calcd for $C_{53}H_{63}FO_4S_4$ (%): C, 69.85; H, 6.97; found (%): C, 69.67; H, 6.84. ^{1}H NMR (400 MHz, $CDCl_3$, TMS), δ (ppm): 7.71–7.69 (br, 2H), 7.47–7.45 (br, 4H), 7.08–7.06 (br, 4H), 4.26–4.24 (br, 2H), 3.95–3.93 (br, 4H), 1.82–1.80 (br, 3H), 1.30–1.28 (br, 23H), 0.99–0.86 (br, 22H). **PTB7-Th** was synthesized with the similar procedure.

Instruments and measurements

^{1}H nuclear magnetic resonance (^{1}H NMR) spectra were measured on an Agilent arx-400 spectrometer. Elemental analysis was carried out on a flash EA1112 analyzer. UV-Vis absorption spectra were measured by using an Agilent Carry-5000 UV-Vis spectrophotometer. Electrochemical cyclic voltammetry (CV) was performed on a Zahner Zennium electrochemical workstation with a three-electrode system in 0.1 mol L^{-1} Bu_4NPF_6 acetonitrile solutions at a scan rate of 50 mV s^{-1}. The three-electrode system included a Pt disk, Pt plate, and Ag/Ag^+ electrode as the working electrode, counter electrode and reference electrode, respectively. The potential of the Ag/Ag^+ reference electrode was internally calibrated by using the ferrocene/ferrocenium redox couple (Fc/Fc^+), and the Ag/Ag^+ reference electrode possessed an energy level of −4.71 eV. The molecular weight of the polymer was measured by the GPC

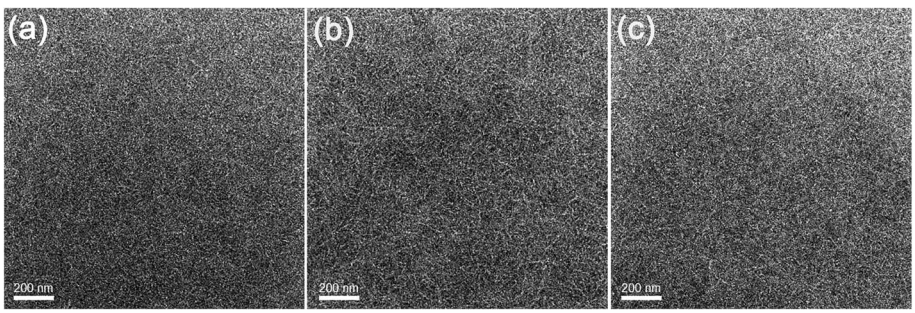

Fig. 5 TEM images of **PBTF-OP**:$PC_{71}BM$ blend films: (a) without DIO, (b) with 1.5% DIO additive treatment and (c) with 3% DIO additive treatment.

method with polystyrene as the standard and 1,2,4-tricholorobenzene as the solvent at 160 °C using an Agilent Technologies PL-GPC220. Thermogravimetric analysis (TGA) was performed on a Discovery TGA from TA Instruments Inc. under a nitrogen atmosphere. X-ray diffraction (XRD) measurements were performed using a Bruker D8 Advance Instrument at 40 kV voltage and 200 mA current with Cu Kα radiation. The atomic force microscopy (AFM) measurements of the surface morphology of the samples were conducted on a Dimension 3100 (Veeco) Atomic Force Microscope in the tapping mode. Transmission electron microscopy (TEM) was performed on a Tecnai G2 F20 S-TWIN instrument at 200 kV accelerating voltage. The current–voltage (*J–V*) measurements of the devices were conducted on a computer-controlled Keithley 2450 Source Measure Unit. The power conversion efficiencies of the PSCs were measured under AM 1.5G illumination (100 mW cm^{-2}) using a SS-F5-3A (Enli Technology Co. Ltd.) solar simulator (AAA grade, 50 mm × 50 mm photo-beam size). EQE measurements were performed at a Solar Cell Spectral Response Measurement System QE-R3011 (Enli Technololy Co. Ltd.). The light intensity at each wavelength was calibrated with a standard single-crystal Si photovoltaic cell. The thickness of the photoactive layer was measured by using a KLA-Tencor D-100 (KLA-Tencor Inc.).

Device fabrication

The PSCs were fabricated with the structure of ITO/PEDOT:PSS/polymer:$PC_{71}BM$/Ca/Al. The ITO-coated glass substrate was cleaned in an ultrasonic bath with deionized water, acetone, and isopropanol. Subsequently, the pre-cleaned ITO-coated glass substrate was treated by using UV-ozone for 20 min. A poly(3,4-ethylenedioxythiophene):poly(styrenesulfonate) (PEDOT:PSS) solution (Clevious P VP AI 4083, H. C. Stark, Germany) was then spin-coated onto the pre-cleaned ITO coated glass substrates, and then dried by baking in an oven at 150 °C for 15 min to get PEDOT:PSS films with a thickness of ~40 nm. The photosensitive blend layer was prepared by spin coating the *o*-dichlorobenzene solution of polymer and $PC_{71}BM$ on the PEDOT:PSS layer. And then, 20 nm Ca and 100 nm Al was thermally deposited in a vacuum under a pressure of 4×10^{-4} Pa. Except for the deposition of the PEDOT:PSS layers, all the other fabrication processes were carried out inside a controlled atmosphere of a nitrogen dry box containing less than 10 ppm oxygen and moisture. The effective area of one cell is 4 mm^2.

Acknowledgements

This work was supported by the National Natural Science Foundation of China (NSFC) (No. 91333204, 51203168, 51422306, 51503135 and 51573120), the Priority Academic Program Development of Jiangsu Higher Education Institutions, the Jiangsu Provincial Natural Science Foundation (Grant No. BK20150332), the Natural Science Foundation of the Jiangsu Higher Education Institutions of China (Grant No. 15KJB430027) and the Ministry of Science and Technology of China (973 project, No. 2014CB643501). Wanbin Li and Bing Guo contributed equally to this work.

References

1 (*a*) G. Yu, J. Gao, J. C. Hummelen, F. Wudl and A. J. Heeger, *Science*, 1995, **270**, 1789; (*b*) A. J. Heeger, *Chem. Soc. Rev.*, 2010, **39**, 2354; (*c*) L. Dou, Y. Liu, Z. Hong, G. Li and Y. Yang, *Chem. Rev.*, 2015, **115**, 12633.
2 (*a*) Y. Huang, E. J. Kramer, A. J. Heeger and G. C. Bazan, *Chem. Rev.*, 2014, **114**, 7006; (*b*) K. A. Mazzio and C. K. Luscombe, *Chem. Soc. Rev.*, 2015, **44**, 78; (*c*) Z. He, H. Wu and Y. Cao, *Adv. Mater.*, 2014, **26**, 1006.
3 (*a*) L. Lu, T. Zheng, Q. Wu, A. M. Schneider, D. Zhao and L. Yu, *Chem. Rev.*, 2015, **115**, 12666; (*b*) C. H. Cui, J. Min, C.-L. Ho, T. Ameri, P. Yang, J. Z. Zhao, C. J. Brabec and W.-Y. Wong, *Chem. Commun.*, 2013, **49**, 4409.
4 (*a*) G. Li, R. Zhu and Y. Yang, *Nat. Photonics*, 2012, **6**, 153; (*b*) M. T. Dang, L. Hirsch, G. Wantz and J. D. Wuest, *Chem. Rev.*, 2013, **113**, 3734; (*c*) Y. Liu, Z. A. Page, T. P. Russell and T. Emrick, *Angew. Chem., Int. Ed.*, 2015, **54**, 11485.
5 (*a*) F. C. Krebs, N. Espinosa, M. Hösel, P. R. Søndergaard and M. Jørgensen, *Adv. Mater.*, 2014, **26**, 29; (*b*) C. H. Cui and W.-Y. Wong, *Macromol. Rapid Commun.*, 2016, **37**, 287; (*c*) C. H. Cui, Z. C. He, Y. Wu, X. Cheng, H. B. Wu, Y. F. Li, Y. Cao and W.-Y. Wong, *Energy Environ. Sci.*, 2016, **9**, 885.
6 (*a*) W. Li, A. Furlan, K. H. Hendriks, M. M. Wienk and R. A. J. Janssen, *J. Am. Chem. Soc.*, 2013, **135**, 5529; (*b*) X. Guo, C. H. Cui, M. J. Zhang, L. J. Huo, Y. Huang, J. H. Hou and Y. F. Li, *Energy Environ. Sci.*, 2012, **5**, 7943.
7 (*a*) T. Basel, U. Huynh, T. Zheng, T. Xu, L. Yu and Z. V. Vardeny, *Adv. Funct. Mater.*, 2015, **25**, 1895; (*b*) V. D. Mihailetchi, J. K. Duren, J. P. W. M. Blom, J. C. Hummelen, R. A. J. Janssen, J. M. Kroon, M. T. Rispens, W. J. H. Verhees and M. M. Wienk, *Adv. Funct. Mater.*, 2003, **13**, 43; (*c*) A. J. Heeger, *Adv. Mater.*, 2014, **26**, 10.
8 M. J. Zhang, X. Guo and Y. F. Li, *Adv. Energy Mater.*, 2011, **1**, 557.
9 (*a*) H. Zhang, L. Ye and J. Hou, *Polym. Int.*, 2015, **64**, 957; (*b*) Z. C. He, C. M. Zhong, X. Huang, W.-Y. Wong, H. B. Wu, L. W. Chen, S. J. Su and Y. Cao, *Adv. Mater.*, 2011, **23**, 4636.
10 Z. G. Zhang and Y. F. Li, *Sci. China: Chem.*, 2015, **58**, 192.
11 Y. F. Li, *Acc. Chem. Res.*, 2012, **45**, 723.
12 (*a*) J. Peet, A. J. Heeger and G. C. Bazan, *Acc. Chem. Res.*, 2009, **42**, 1700; (*b*) J. K. Lee, W. L. Ma, C. J. Brabec, J. Yuen, J. S. Moon, J. Y. Kim, K. Lee, G. C. Bazan and A. J. Heeger, *J. Am. Chem. Soc.*, 2008, **130**, 3619.
13 (*a*) W. Ma, J. Reinspach, Y. Zhou, Y. Diao, T. McAfee, S. C. B. Mannsfeld, Z. Bao and H. Ade, *Adv. Funct. Mater.*, 2015, **25**, 3131; (*b*) M. J. Zhang, X. Guo, W. Ma, H. Ade and J. Hou, *Adv. Mater.*, 2015, **27**, 4655; (*c*) W. Ma, J. Tumbleston, M. Wang, E. Gann, F. Huang and H. Ade, *Adv. Energy Mater.*, 2013, **3**, 864.
14 S. H. Liao, H. J. Jhuo, P. N. Yeh, Y. S. Cheng, Y. L. Li, Y. H. Lee, S. Sharma and S. A. Chen, *Sci. Rep.*, 2014, **4**, 6813.
15 Z. He, B. Xiao, F. Liu, H. Wu, Y. Yang, S. Xiao, C. Wang, T. P. Russell and Y. Cao, *Nat. Photonics*, 2015, **9**, 174.
16 J. Huang, C.-Z. Li, C.-C. Chueh, S.-Q. Liu, J.-S. Yu and A. K. Y. Jen, *Adv. Energy Mater.*, 2015, **5**, 1500406.

17 Y. Liu, J. Zhao, Z. Li, C. Mu, W. Ma, H. Hu, K. Jiang, H. Lin, H. Ade and H. Yan, *Nat. Commun.*, 2014, **5**, 5293.
18 H. Lin, S. Chen, Z. Li, J. Y. L. Lai, G. Yang, T. McAfee, K. Jiang, Y. Li, Y. Liu, H. Hu, J. Zhao, W. Ma, H. Ade and H. Yan, *Adv. Mater.*, 2015, **27**, 7299.
19 L. Nian, W. Zhang, N. Zhu, L. Liu, Z. Xie, H. Wu, F. Würthner and Y. Ma, *J. Am. Chem. Soc.*, 2015, **137**, 6995.
20 S. Q. Zhang, L. Ye, W. C. Zhao, B. Yang, Q. Wang and J. H. Hou, *Sci. China: Chem.*, 2015, **58**, 248.
21 L. Ye, S. Zhang, L. Huo, M. Zhang and J. Hou, *Acc. Chem. Res.*, 2014, **47**, 1595.
22 H. Yao, H. Zhang, L. Ye, W. Zhao, S. Zhang and J. Hou, *Macromolecules*, 2015, **48**, 3493.
23 K. Sun, Z. Xiao, S. Lu, W. Zajaczkowski, W. Pisula, E. Hanssen, J. M. White, R. M. Williamson, J. Subbiah, J. Y. Ouyang, A. B. Holmes, W. W. H. Wong and D. J. Jones, *Nat. Commun.*, 2015, **6**, 6013.
24 C. Duan, A. Furlan, J. J. Franeker, R. E. M. Willems, M. M. Wienk and R. A. J. Janssen, *Adv. Mater.*, 2015, **27**, 4461.
25 R. Po, G. Bianchi, C. Carbonera and A. Pellegrino, *Macromolecules*, 2015, **48**, 453.
26 (*a*) L. Huo, J. Hou, S. Zhang, H.-Y. Chen and Y. Yang, *Angew. Chem., Int. Ed.*, 2010, **49**, 1500; (*b*) L. Huo, S. Zhang, X. Guo, F. Xu, Y. Li and J. Hou, *Angew. Chem., Int. Ed.*, 2011, **50**, 9697; (*c*) M. J. Zhang, X. Guo, S. Zhang and J. Hou, *Adv. Mater.*, 2014, **26**, 1118.
27 (*a*) B. C. Thompson and J. M. J. Fréchet, *Angew. Chem., Int. Ed.*, 2008, **47**, 58; (*b*) W.-Y. Wong and C.-L. Ho, *Acc. Chem. Res.*, 2010, **43**, 1246.
28 P. W. M. Blom, V. D. Mihailetchi, L. J. A. Koster and D. E. Markov, *Adv. Mater.*, 2007, **19**, 1551.
29 Y. J. He, H. Y. Chen, J. H. Hou and Y. F. Li, *J. Am. Chem. Soc.*, 2010, **132**, 1377.
30 M. J. Zhang, X. Guo, W. Ma, S. Zhang, L. Huo, H. Ade and J. Hou, *Adv. Mater.*, 2014, **26**, 2089.
31 W. Chen, Z. Du, L. Han, M. Xiao, W. Shen, T. Wang, Y. Zhou and R. Yang, *J. Mater. Chem. A*, 2015, **3**, 3130.
32 M. J. Zhang, Y. Gu, X. Guo, F. Liu, S. Zhang, L. Huo, T. P. Russell and J. Hou, *Adv. Mater.*, 2013, **25**, 4944.
33 Q. Sun, H. Wang, C. Yang and Y. F. Li, *J. Mater. Chem.*, 2003, **13**, 800.
34 J. Hou, Z. Tan, Y. Yan, Y. He, C. Yang and Y. F. Li, *J. Am. Chem. Soc.*, 2006, **128**, 4911.
35 M. J. Zhang, X. Guo, W. Ma, H. Ade and J. Hou, *Adv. Mater.*, 2014, **26**, 5880.
36 Y. Y. Liang, Z. Xu, J. B. Xia, S.-T. Tsai, Y. Wu, G. Li, C. Ray and L. P. Yu, *Adv. Mater.*, 2010, **22**, E135.
37 V. Tamilavan, K. H. Roh, R. Agneeswari, D. Y. Lee, S. Cho, Y. Jin, S. H. Park and M. H. Hyun, *J. Mater. Chem. A*, 2014, **2**, 20126.
38 X. Guo, M. Zhang, W. Ma, L. Ye, S. Zhang, S. Liu, H. Ade, F. Huang and J. Hou, *Adv. Mater.*, 2014, **26**, 4043.
39 C. H. Cui, W.-Y. Wong and Y. F. Li, *Energy Environ. Sci.*, 2014, **7**, 2276.